

## Magneto-rheological and passive damper combinations for seismic mitigation of building structures

Nivithigala P.K.V. Karunaratne<sup>\*</sup>, David P. Thambiratnam<sup>a</sup> and Nimal J. Perera<sup>b</sup>

*School of Civil Engineering and Built Environment, Science & Engineering Faculty, Queensland University of Technology, Brisbane, Australia*

*(Received February 15, 2016, Revised May 6, 2016, Accepted August 19, 2016)*

**Abstract.** Building structures generally have inherent low damping capability and hence are vulnerable to seismic excitations. Control devices therefore play a useful role in providing safety to building structures subject to seismic events. In recent years semi-active dampers have gained considerable attention as structural control devices in the building construction industry. Magneto-rheological (MR) damper, a type of semi-active damper has proven to be effective in seismic mitigation of building structures. MR dampers contain a controllable MR fluid whose rheological properties vary rapidly with the applied magnetic field. Although some research has been carried out on the use of MR dampers in building structures, optimal design of MR damper and combined use of MR and passive dampers for real scale buildings has hardly been investigated.

This paper investigates the use of MR dampers and incorporating MR-passive damper combinations in building structures in order to achieve acceptable levels of seismic performance. In order to do so, it first develops the MR damper model by integrating control algorithms commonly used in MR damper modelling. The developed MR damper is then integrated in to the seismically excited structure as a time domain function. Linear and nonlinear structure models are evaluated in real time scenarios. Analyses are conducted to investigate the influence of location and number of devices on the seismic performance of the building structure. The findings of this paper provide information towards the design and construction of earthquake safe buildings with optimally employed MR dampers and MR-passive damper combinations.

**Keywords:** seismic engineering; energy dissipation; magneto-rheology; visco-elastic; friction; dampers

### 1. Introduction

Earthquakes generate seismic waves that can lead to the destruction of manmade structures with catastrophic outcomes. Since 1900, an average of 18 major earthquakes (magnitude 7.0-7.9) and one larger earthquake (magnitude 8.0 or more) have occurred annually. While this average has been relatively stable, long-term prediction of earthquakes is difficult making it critical to construct buildings to withstand credible seismic excitations.

---

<sup>\*</sup>Corresponding author, Ph.D., E-mail: [karunaratnekasun@yahoo.com](mailto:karunaratnekasun@yahoo.com)

<sup>a</sup>Professor, E-mail: [d.thambiratnam@qut.edu.au](mailto:d.thambiratnam@qut.edu.au)

<sup>b</sup>Adjunct Professor, E-mail: [nimal.perera@robertbird.com.au](mailto:nimal.perera@robertbird.com.au)

Under seismic excitations, energy dissipative devices work by absorbing a portion of the input energy that would be transmitted to the structure. According to the law of conservation of energy, the energy equation can be expressed as

$$E = E_k + E_s + E_h + E_d \quad (1)$$

Where,  $E$  is the total input energy from earthquake motion,  $E_k$  is the absolute kinetic energy,  $E_s$  is the recoverable elastic energy,  $E_h$  is the irrecoverable energy dissipated by the structural system through inelastic deformation,  $E_d$  is the damping energy dissipated by inherent structural damping and supplemental damping devices. Since inherent damping of the structure is very low, the energy dissipated through elastic region is also very low. Energy dissipation through inherent structural damping is mainly caused by thermal effects when solids deform. The integration of a supplemental damping device would hence be a suitable option for energy dissipation of the building. Investigation of such systems is crucial in the current earthquake resistant building design practice.

Over the years, numerous supplemental damping systems have been proposed. These structural control solutions are further been developing with new technological advances. Commonly used structural control systems include base isolation, passive energy dissipation, active energy dissipation and semi-active control strategies. Base isolation becomes expensive when the building sizes increases. Passive devices (dampers) have limited capacity and are unable to adapt to external loading conditions. Active and hybrid devices are able to vary according to the external loading conditions, yet require a large power supply which might not be available at all times, especially during a seismic event. These challenges are well addressed by semi-active systems. They use the measured structural response to determine the required control forces. Magneto-Rheological (MR) damper, a specific semi-active device, has gained significance due to its high damping capacity, less power requirement, mechanical simplicity and greater performance index in mitigating structural seismic response. These unique features of semi-active MR damper systems have attracted researches and engineers to study the feasibility of using them in building structures.

Research on single and hybrid damper types has been reasonably well carried out (Hao and Zhang 2016), (Lee and Kim 2015). But there is a lag in developing combined damper systems with the MR damper. This research develops a procedure for using MR dampers alone and in conjunction with visco-elastic and friction dampers to provide the required amount of seismic mitigation in building structures. The procedure is illustrated through its application to an 18 storey and 12 storey steel building structures. Results confirm the feasibility of the procedure developed in this research.

## 2. Damper modelling and integration

Prior to the integration of dampers into the considered building, dampers need to be modelled and verified with the existing experimental and numerical results.

### 2.1 Numerical simulation procedure

Three different damper systems have been used in this study, MR damper, visco-elastic damper

and friction damper. Each of them is individually modelled and later combined into take the combined damper systems.

### 2.1.1 MR dampers

MR damper behaviour can be well explained by a mathematical model which describes the nonlinear hysteretic behaviour. Since MR damper uses measured structural response to determine the required control force, it caters to varying external loading conditions. The MR damper herein has a maximum capacity of 1700 kN. Damping characteristics of an MR damper are governed by the current applied to the electromagnet. Structure response, applied current and damper forces therefore work simultaneously in the MR damper modelling.

Modelling the MR damper consists of two basic steps, MR damper controller and MR force generator. Schematic diagram of the system is shown in Fig. 2.1.

#### 1. MR damper controller

MR damper is controlled by the current generated by the controller. To do so, control force signals need to be converted into current signals to operate the MR damper. Two approaches are preferred, using an inverse model of the MR damper or using an algorithm which converts control forces into current signal.

MR damper can be used either in passive or semi-active mode for the control of a structure. A constant current is supplied to the MR damper while it is in the passive mode. Feedback data is not generated for the controller and damper force is generated passively for the given current. The semi-actively controlled MR damper system uses feedback data along with sensors and controllers. The General definition for a semi-actively control device is that it is a device with properties which do not input energy into the system that is being controlled. In MR dampers it is the current going into the damper which controls the damper force. This current can change the magnitude of damper force by changing the intensity of the magnetic flux from the electromagnetic coil, but it cannot change the direction of the damper force in a given state, like an active controller.

#### 2. MR damper force generator

To determine the appropriate control force, a semi-active controller involves the use of optimal control theory along with feedback data collected from sensors such as accelerometers, load cells, displacement transducers, etc. This model is also known as a MR damper forward model.

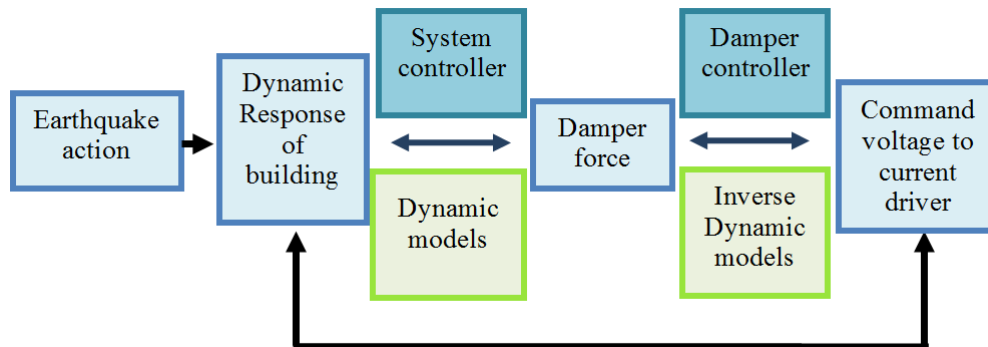


Fig. 2.1 Schematic diagram of MR damper system

In order to evaluate the performance of the MR system and MR-passive damper systems, computer models are formulated based on the equations of motion for the dynamic systems. These equations of motion are written in state-space form which benefits this simulation because the MATLAB Simulink Dynamic System Simulator (TheMathWorksInc. 2014) is capable of processing the ordinary differential equations at real-time speeds (Das *et al.* 2012).

### 2.1.2 Viscoelastic dampers

A viscoelastic damper is modelled as a linear spring and dash-pot in parallel. In this model, the spring represents stiffness and the dashpot represents damping. Abbas and Kelly (1994) defined the stiffness and damping coefficients as follows

$$k_d = \frac{G'A}{t} \quad (2)$$

$$C_d = \frac{G''A}{\omega t} \quad (3)$$

$A$  = Shear area of the VE material

$t$  = Thickness of the VE material

$\omega$  = Loading frequency of the VE damper

$G'$  = Shear storage modulus

$G''$  = Shear loss modulus

$$G' = 16\omega^{0.51}\gamma^{-0.23}e^{(72.46/Temp)} \quad (4)$$

$$G'' = 18.5\omega^{0.51}\gamma^{-0.20}e^{(73.89/Temp)} \quad (5)$$

$\gamma$  = Shear Strain

Linear viscoelastic model as a function of strain is introduced in MATLAB dynamic solver. Temperature is kept constant at 24°C during the analysis. Values for  $k_d$  is taken as 10,000 kN/m and  $c_d$  is taken as 63000 kN/m.

### 2.1.3 Friction dampers

Frictional contact was introduced using a Coulomb friction element in which the energy is absorbed via sliding friction. Friction generated by the relative motion of the two surfaces that press against each other and convert the kinetic energy of the system into heat.

Most commonly used friction model is the Coulomb friction model. This can be formulated as

$$F = \begin{cases} F_c \sin(v) & \text{if } v > 0 \\ F_{app} & \text{if } v = 0 \text{ and } F_{app} < F_c \end{cases} \quad (6)$$

where  $F$  is the friction force,  $v = \dot{x}$  the sliding speed and  $F_{app}$  is the applied force on the body,  $F_c$  is the Coulomb sliding friction force.

Numerical simulation of the system with friction damper was carried out in Matlab Simulink environment. Coulomb friction model assumes that zero relative motion occurs until frictional stress reaches critical stress, which is proportional to the contact pressure. The contact problem is therefore in the linear range, since all the states are governed by linear equations.

#### 2.1.4 Combined damper systems

Although MR damper works better compared to passive and active dampers, the associate cost is relatively high. In order to maintain a sustain nature of the seismic mitigation technique author proposed combine use of passive dampers with MR dampers. Passive dampers are reliable and cost effective compared to active dampers and cooperate with MR dampers without coupling complications. Two different damper combinations are used in the study.

1. Combined Friction - MR damper system
2. Combined Viscoelastic - MR damper system

Performance of the friction damper is better when it is installed in the upper floors while VE damper performs better when installed in the lower floors (Marko, Thambiratnam, & Perera, 2004). The selection of damper placement is hence decided according to the previous passive damper based research. Accordingly, MR damper is kept in the lower floors to obtain the best seismic performance of the building.

#### 2.2 Integration of MR Damper into buildings

State space representation of the equation of motion for a dynamic system is used in the study. The dynamic systems are described by ordinary differential equations where time is the independent variable. By using vector-matrix notations, an  $n^{\text{th}}$ -order differential equation may be expressed by a first order vector-matrix differential equation (Dyke *et al.* 1996)

$$\dot{X} = AX + BU \quad (7)$$

$$Y = CX + DU \quad (8)$$

Where,  $X$  is the state vector and  $\dot{X}$  denotes differentiation of  $X$  with respect to time.  $A$ ,  $B$ ,  $C$ ,  $D$  are state space matrices.  $U$  is the vector of the measured control forces and  $Y$  is the measured output.

Since the floor slab is assumed to be rigid in the horizontal plane, all the nodes associated with each floor have the same horizontal displacements. This assumption can be used in writing constraint equations relating the dependent horizontal DOFs on each floor slab to a single active horizontal DOF and using a Ritz transformation (Craig and Yung-Tsen 1982).

In this research the Clipped Optimal Control algorithm is used as the damper controller. When the building is subjected to dynamic loading, the building model delivers the velocity and displacement response of the floor mass to a current controller and to a numerical MR damper model, which then calculates and feeds back the damper resistance force to the equation of motion for next step calculation.

The controller designed for this study was verified with the control design model of the structure of interest. This was completely modelled in a MATLAB/Simulink environment. A state-space model of the structure was placed in a Simulink block with inputs of ground motion excitation and damper force. The outputs of this block are displacements, velocities and accelerations, the last of which were fed into the controller block containing the state-space model of the controller. For the purpose of obtaining the correct response values converted in to an electronic signal, high fidelity sensors are used. The controller block then feeds the desired force into a MR damper model. Finally the control device feeds the actual damper forces back into the structure. The benefit of semi-active control was shown during the analysis. For the stories in which passive on or passive off control seemed to perform better for any given event, semi-active

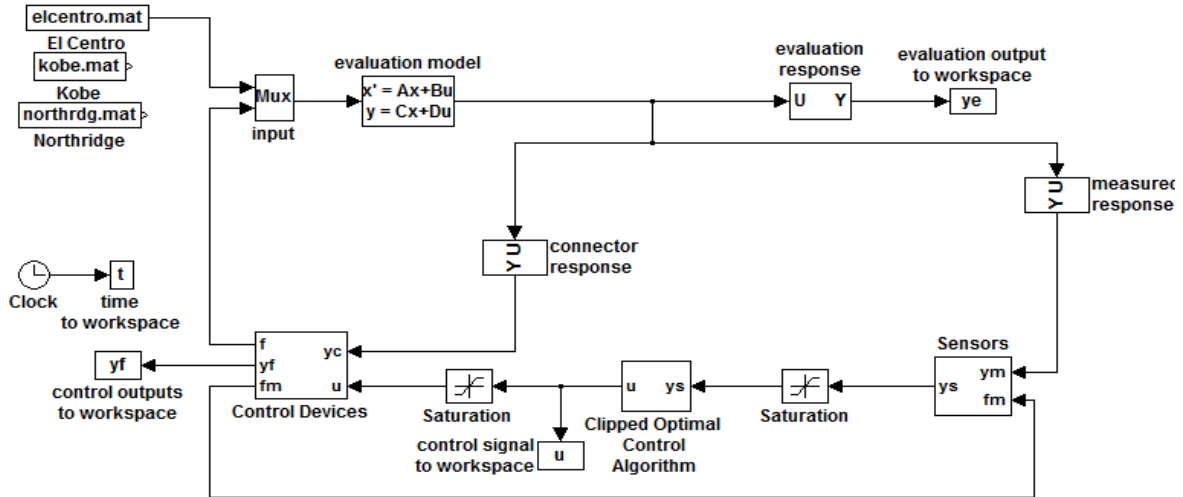


Fig. 2-2 Simulink model for structural simulation with MR damper

control seemed to provide the better performance at each story while creating a more congruent inter-story drift across all floors. This paper only shows the results for passive on case of the MR damper and tip deflection and acceleration results as evaluation parameters in order to study the general behaviour of the system.

In order to effectively use the MATLAB-Simulink model to building structures, recently introduced structural tool by CSI (CSI 2013), SAP2000-OAPI is used in this research. The SAP2000 Open Application Programming Interface (OAPI) is a programming tool which aims to offer efficient access to the analysis and design technology of the SAP2000 structural analysis software, by allowing, during run-time, a direct bind to be established, between a third-party application and the analysis software itself. Simulations are carried out in SAP2000 OAPI, where both Simulink damper model and SAP2000 finite element model run simultaneously in a time domain.

### 3. Methodology

#### 3.1 Analytical approach

A dynamic system consisting of a finite number of lumped elements may be described by ordinary differential equations in which time is the independent variable.

MR Damper force provides resistance for the structure against the seismic excitation force. It is assumed that the MR damper resistant force  $f_d$  is adequate to keep the structure in the linear region. Therefore equation of motion for a system needs to be modified accordingly to include the damper force

$$[m]\ddot{x} + [c]\dot{x} + [k]x = -[\Lambda][m]\ddot{x}_g - [\Gamma] f_d x \quad (9)$$

where,  $[\Gamma]$  is the MR damper placement matrix,

The corresponding state space form will be

$$\begin{bmatrix} \dot{x} \\ \dot{\dot{x}} \end{bmatrix} = \begin{bmatrix} I & 0 \\ 0 & I \\ -[m]^{-1}[k] & -[m]^{-1}[c] \end{bmatrix} \begin{bmatrix} x \\ \dot{x} \end{bmatrix} + \begin{bmatrix} 0 \\ 0 \\ -[\Lambda]\ddot{x}_g - [m]^{-1}[\Gamma] f_d \end{bmatrix} \quad (10)$$

In order to compare MR damper effect for a system, Simulink model was developed and the system response was observed. System without any external damper, system with increased inherent damping and a system with MR damping were compared.

**Clipped optimal control algorithm**

MR Damper requires a proper control to generate the damping force effectively. Force produced by the MR damper cannot be directly controlled. The voltage or current controls the MR damper force according to the response of the structure. Based on this observation, the following guidelines were used to develop the control algorithm (Metwally *et al.* 2006).

- The control voltage to the  $i^{\text{th}}$  device is restricted to the range  $V_i = [0, V_{max}]$
- For a fixed set of status, the magnitude of the applied force increases when  $V_i$  increases, and decreases when  $V_i$  decreases.

Clipped optimal control (Tseng and Hedrick 1994) is proposed by (Dyke *et al.* 1996). The aim is to design a linear optimal controller  $K_c$  which calculates a vector of desired control forces,  $f_c = [f_{c1} \ f_{c2} \ \dots \ f_{cn}]^T$  based on the measured structural response  $Y$  and the measured control forces vector  $f_d$  applied to the structure

$$f_c = L^{-1} \left\{ -K_c L \begin{Bmatrix} Y \\ f_d \end{Bmatrix} \right\} \quad (11)$$

where,  $L\{ \cdot \}$  is the Laplace transform.

The algorithm for selecting the command signal for  $i^{\text{th}}$  value of MR damper can be written as

$$V_i = V_{max} H((f_c - f_i) f_i) \quad (12)$$

- $V_{max}$  - maximum voltage applied to the current driver (with saturation of magnetic field)
- $f_c$  - desired optimal force
- $f_i$  - force produced by the  $i^{\text{th}}$  MR damper
- $H$  - Heaviside step function

This algorithm commanded the voltage  $V_i$  as follows. When the MR damper is providing the desired optimal force, the voltage applied to the damper should remain at the present level. If the magnitude of the force produced by the MR damper is smaller than the magnitude of the optimal force and the two forces have the same sign, the voltage applied to the current driver is increased to the maximum. Otherwise the command voltage is set to zero.

Acceleration feedback control strategies based on H1/LQG methods are employed to design the optimal controller. There are different control algorithms used in different studies. Amini and Javanbakht (2014) recently developed neural network inverse model to translate the desired control force into an applicable MR damper command voltage.

The MR damper is then successfully integrated to a finite element technique and assigned a parallel analysis path to obtain the required results. SAP2000 OAPI provides the communicating platform. Three different earthquake signals have been chosen. In both scenarios, single MR damper in a building and a damper group in a building are successfully validated.

### 3.2 Modelling of the structures

18 storey 2D frame with 3 bays and 12 storey 2D frame with 3 bays are considered in the study. In each building stories are 4 m high with moment resisting frames providing the lateral load resistance. Bays are at 6 m centres. Columns are of 450 MPa steel having 0.4 m×0.4 m cross-section. W30×99 sections of 250 MPa steel wide flange beams are used in the models. The seismic mass of each floor (expressed as a weight force) is  $5 \times 10^5$  kN. This includes the mass of the steel frame, floor slabs, partitions, ceiling, mechanical and electrical services and the roof.

Following assumptions are applied to the structure model,

1. Floors are rigid and the total mass is concentrated at the levels of the floors.
2. There is no rotation about the horizontal axis.
3. Vertical component of the acceleration is neglected. Structure is only subjected to horizontal acceleration.

Earthquake acceleration is applied in the 'x' direction at the base of the structure. The support at the base is restrained against translation in 'y' direction and rotation about 'z' axis.

Three earthquake excitations have been considered for the analysis:

- i. El Centro - The N-S component recorded at the Imperial Valley Irrigation District substation in El Centro, California, during the Imperial Valley, California earthquake of May, 18, 1940.
- ii. Kobe. The N-S component recorded at the Kobe Japanese Meteorological Agency (JMA) station during the Hyogo-ken Nanbu earthquake of January 17, 1995
- iii. Northridge. The N-S component recorded at Sylmar County Hospital parking lot in Sylmar, California, during the Northridge, California earthquake of January 17, 1994.

Simulations are carried out to determine the response of the structure fitted with the MR damper and MR-passive combinations. The efficiency of a damper system is investigated according to the type of the dampers used and the locations where they have been installed in the building. Thereafter generalized seismic response reduction patterns are modelled for particular building and for the considered damping systems. These patterns could be used to identify the optimum damping placement and damping values associated with a specific damper or a damper system.

## 4 Results and discussion

### 4.1 18 storey 2D structure

The combination of MR and passive dampers is used to provide seismic mitigation of an 18 storey steel frame structure. Three main damping systems are used. The first system consists of MR dampers only. A single MR damper and two MR dampers are installed separately in the building to monitor its seismic response. Combined MR-Viscoelastic damper system is the second system consisting of one MR damper and one VE damper. As the third one, combined MR-Friction damper system is used. Each damping system is analysed for different damper locations. Seismic analyses are performed with one type of damper at one placement at a time. Effectiveness of each damper system was investigated for the three different earthquake excitations. Tip deflection and tip acceleration are taken as key evaluation parameters. The influence of damper system and its placement were investigated for establishing the optimum combination.

Table 4-1 Tip deflection and tip acceleration of the un-damped structure

	El Centro	Kobe	Northridge
Tip Deflection(m)	0.341	0.192	0.319
Tip Acceleration(ms <sup>-2</sup> )	5.49	4.76	5.83

4.1.1 Un-controlled structure

The un-controlled structure is modelled and analysed first. The seismic response parameters are used to compare the damped results. Tip deflection and tip acceleration results for the un-damped structure are shown in Table 4-1.

Results for tip deflection and tip acceleration reductions obtained for the structure fitted with each damper system at different locations for each of the three earthquake excitations are presented in Section 4.1.2.

4.1.2 Structure fitted with single MR damper only

Fig. 4-1 and Fig. 4-2 show tip deflection and tip acceleration under El-Centro earthquakes when a single MR damper is fitted in the first floor. These figures clearly illustrate the influence of dampers in reducing the seismic response parameters.

The MR damper reduces the tip deflection of the structure by as much as a maximum of 23.86% under El-Centro earthquake excitation. Analyses are conducted for different damper types and placements for different earthquake excitations. Tip deflection and tip acceleration results for un-damped and damped structures under different MR damper placements are tabulated in Table 4-2. According to that, it can be concluded that a single MR damper significantly affects the seismic response parameters. Both tip deflection and tip accelerations are reduced by 18-25% when it is placed in 1st storey. The reduction gradually decreases when the damper placement reaches upper levels, but the reduction is consistent for all earthquake accelerations. It can therefore be concluded that the MR damper performed well when it is placed at the lower levels of the building.

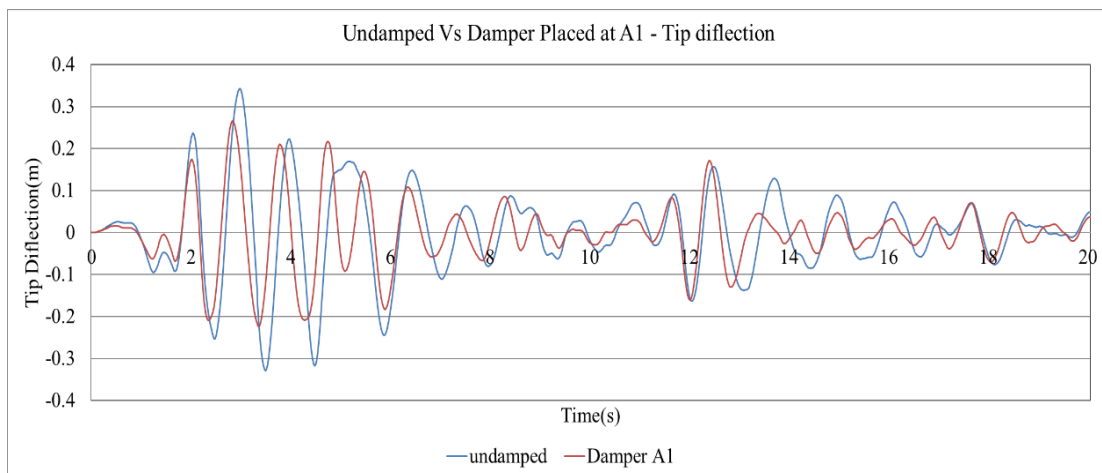


Fig. 4-1 Tip deflection response of the un-damped structure and structure fitted with MR damper in first floor under El Centro earthquake

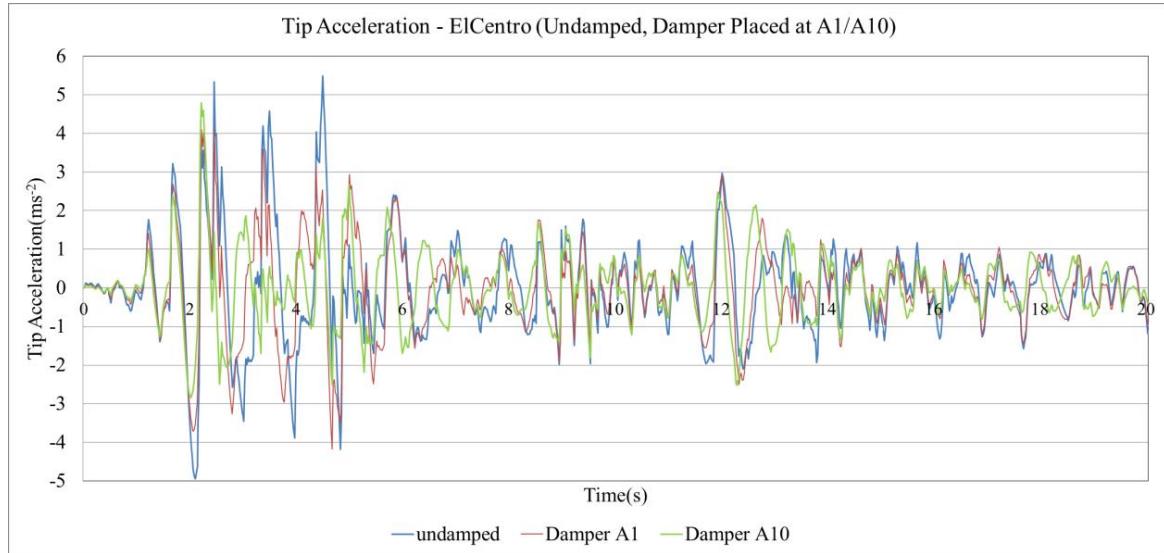


Fig. 4-2 Tip acceleration response comparison of un-damped, damper embedded in 1st, 10th floors under El-Centro earthquake

Table 4-2 Seismic response reduction using single MR damper

Earthquake	Damper Placement	Tip Deflection (m)		Reduction (%)	Tip Acceleration (ms <sup>-2</sup> )		Reduction (%)
		Un-damped	Damped		Un-damped	Damped	
El-Centro	A1	0.341	0.265	22.29	5.49	4.18	23.86
	A3		0.289	15.25		4.43	19.31
	A7		0.302	11.44		4.67	14.94
	A10		0.309	9.38		4.79	12.75
	A13		0.294	13.78		4.95	9.84
	A16		0.322	5.57		4.69	14.57
Kobe	A1	0.192	0.164	14.58	4.76	3.52	26.05
	A3		0.171	10.94		3.89	18.28
	A7		0.175	8.85		4.13	13.24
	A10		0.181	5.73		4.32	9.24
	A13		0.176	8.33		4.21	11.55
	A16		0.183	4.69		4.43	6.93
Northridge	A1	0.319	0.254	20.38	5.83	4.78	18.01
	A3		0.271	15.05		4.99	14.41
	A7		0.279	12.54		5.13	12.01
	A10		0.285	10.66		5.42	7.03
	A13		0.277	13.17		5.41	7.20
	A16		0.28	12.23		5.65	3.09

#### 4.1.3 Structure fitted with two MR dampers

According to previous analysis, a better seismic performance is achieved when MR damper is placed in the first floor and it is significant compared to that with other damper placements. In the next part of the study one MR damper is hence always kept in the first floor for the first three analyses and then moved to upper floors for other three. Results are shown in Table 4-3.

Both tip deflection and tip accelerations are reduced up to 30%-40% when two MR dampers are located at the lower floors. Similar to the outcome of Table 4-2, Table 4-3 shows that damper placed in bottom floors show better performance.

#### 4.1.4 Structure fitted with combined MR - VE damper system

In general MR damper performs better compared to a VE damper and hence the MR damper is kept in the lower floor of the structure at all times. Since the VE dampers perform better in the lower and middle part of the structure (Marco *et al.* 2006), damper placements are decided accordingly. Tip deflection and tip acceleration reductions are shown in Table 4.4. Results demonstrate that VE dampers perform better when placed in the lower floors. Overall, the results show good seismic mitigation. But a reduction in the average values is evident compared to the case with two MR dampers.

Table 4-3 Seismic response reduction using two MR dampers

Earthquake	Damper Placement	Tip Deflection (m)		Reduction (%)	Tip Acceleration (ms <sup>-2</sup> )		Reduction (%)
		Undamped	Damped		Undamped	Damped	
El Centro	A1-3		0.212	37.83		3.64	33.70
	A1-5		0.223	34.60		3.81	30.60
	A1-10	0.341	0.231	32.26	5.49	4.10	25.32
	A7-9		0.273	19.94		4.79	12.75
	A10-12		0.287	15.84		4.47	18.58
	A14-16		0.291	14.66		4.67	14.94
Kobe	A1-3		0.119	38.02		3.14	34.03
	A1-5		0.128	33.33		3.32	30.25
	A1-10	0.192	0.131	31.77	4.76	3.53	25.84
	A7-9		0.159	17.19		3.93	17.44
	A10-12		0.168	12.50		3.75	21.22
	A14-16		0.165	14.06		3.98	16.39
Northridge	A1-3		0.202	36.68		4.12	29.33
	A1-5		0.209	34.48		4.35	25.39
	A1-10	0.319	0.221	30.72	5.83	4.49	22.98
	A7-9		0.258	19.12		4.97	14.75
	A10-12		0.253	20.69		5.02	13.89
	A14-16		0.267	16.30		4.89	16.12

Table 4-4 Seismic response reduction using one MR and one VE damper

Earthquake	Damper Placement	Tip Deflection(m)		Reduction	Tip Acceleration(ms <sup>-2</sup> )		Reduction
		Undamped	Damped	(%)	Undamped	Damped	(%)
El Centro	A1-3		0.246	27.86		3.97	27.69
	A1-5		0.259	24.05		3.94	28.23
	A1-10	0.341	0.268	21.41	5.49	4.13	24.77
	A7-9		0.281	17.60		4.61	16.03
	A10-12		0.295	13.49		4.68	14.75
	A14-16		0.304	10.85		4.91	10.56
Kobe	A1-3		0.135	29.69		3.51	26.26
	A1-5		0.142	26.04		3.72	21.85
	A1-10	0.192	0.145	24.48	4.76	3.83	19.54
	A7-9		0.164	14.58		4.12	13.45
	A10-12		0.177	7.81		4.43	6.93
	A14-16		0.181	5.73		4.31	9.45
Northridge	A1-3		0.241	24.45		4.34	25.56
	A1-5		0.249	21.94		4.71	19.21
	A1-10	0.319	0.247	22.57	5.83	4.52	22.47
	A7-9		0.278	12.85		4.99	14.41
	A10-12		0.269	15.67		5.18	11.15
	A14-16		0.291	8.78		5.29	9.26

#### 4.1.5 Structure fitted with combined MR - Friction damper system

Marko *et al.* (2004) stated that friction dampers perform better in the upper floors where the inter-story drifts are maximum. Therefore as in the previous analysis, the MR damper is kept in lower floor while the friction damper is located at the upper floors of the structure. Tip deflection and tip acceleration reductions are shown below. For comparison purposes the same damper locations are maintained as earlier.

According to the above results it can be concluded that the superior performance of the MR damper, the influence of friction damper placement does not seem to be highlighted. Yet compared to other dampers, friction damper reduces tip deflections better when placed in upper floors.

#### 4.1.6 Generalized reduction pattern

Generalized seismic response reduction patterns can be modelled for this particular building and for considered damping systems. These patterns could be used to identify the optimum damping placement and damping values to a specific damper or a damper system.

Four different reduction patterns are developed for this 18 storey structure,

1. Reduction Pattern for single MR damper
2. Reduction Pattern for two MR dampers
3. Reduction Pattern for MR-VE combination
4. Reduction Pattern for MR-Friction combination

Table 4-5 Seismic response reduction using one MR and one Friction damper

Earthquake	Damper Placement	Tip Deflection(m)		Reduction	Tip Acceleration (ms <sup>-2</sup> )		Reduction
		Un-damped	Damped	(%)	Un-damped	Damped	(%)
El Centro	A1-3		0.263	22.87		4.14	24.59
	A1-5		0.262	23.17		4.39	20.04
	A1-10	0.341	0.257	24.63	5.49	4.57	16.76
	A7-9		0.273	19.94		4.71	14.21
	A10-12		0.287	15.84		4.65	15.30
	A14-16		0.271	20.53		4.31	21.49
Kobe	A1-3		0.153	20.31		3.46	27.31
	A1-5		0.167	13.02		3.62	23.95
	A1-10	0.192	0.161	16.15	4.76	4.01	15.76
	A7-9		0.182	5.21		4.12	13.45
	A10-12		0.171	10.94		4.03	15.34
	A14-16		0.159	17.19		3.92	17.65
Northridge	A1-3		0.251	21.32		4.71	19.21
	A1-5		0.274	14.11		4.82	17.32
	A1-10	0.319	0.271	15.05	5.83	4.98	14.58
	A7-9		0.283	11.29		5.12	12.18
	A10-12		0.268	15.99		4.91	15.78
	A14-16		0.261	18.18		5.02	13.89

*Reduction Pattern for single MR damper*

General tip deflection reduction graph for single MR damper according to its placements is shown Fig. 4-4.

According to the graph, tip deflection reduction is exponentially reduced to a certain value and remains same with the increasing height of the placement of the damper. The generalized equation

is given in Eq. (13)

$$f(x) = 9.22 + 17.72e^{-0.32x} \tag{13}$$

Note: Coefficients are obtained with 95% confidence bounds

*Reduction Pattern for two MR dampers*

General tip deflection reduction pattern when two MR dampers are used is shown in Fig. 4-5. 'x' and 'y' axes represent the MR damper 1 and 2 placements respectively, while 'z' axis represents the tip deflection reduction percentage.

The generalized equation for the above graph is given in Eq. (14)

$$f(x, y) = 23.04 - 8.94 \sin(1.14\pi * x * y) - 9.21e^{-(1.83y)^2} \tag{14}$$

Note: Coefficients are obtained with 95% confidence bounds

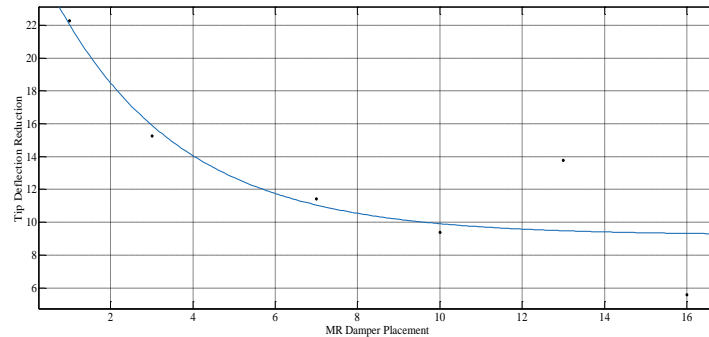


Fig. 4-4 Reduction Pattern for single MR damper

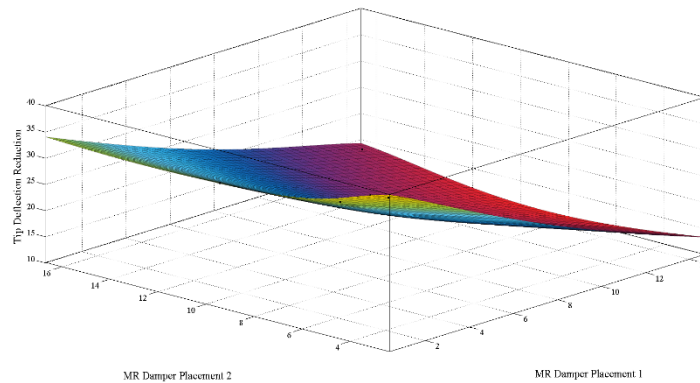


Fig. 4-5 Reduction Pattern for two MR dampers

According to the equation, one MR damper is always needed to be sitting on 1<sup>st</sup> or 2<sup>nd</sup> floor, while other can be moved between 1<sup>st</sup> and 14<sup>th</sup> floor to achieve more than 30% tip deflection reduction. To achieve 25% damping, a single MR damper needs to be installed between the 1<sup>st</sup> and 4<sup>th</sup> floor, while other damper can be located anywhere.

#### *Reduction Pattern for MR-VE combination*

Generalized tip deflection reduction, when using a MR - VE damper combination is shown in Fig. 4-6. 'x' and 'y' axes represent the MR damper and VE damper placements respectively. 'z' axis represents the tip deflection reduction percentage.

The generalized equation for the above graph is given in Eq. (15)

$$f(x, y) = 19.53 - 1.396 \sin(0.681\pi * x * y) + 0.15e^{(-0.95y)^2} \quad (15)$$

Note: Coefficients are obtained with 95% confidence bounds

According to the results, MR damper can be moved across the 1<sup>st</sup> and 4<sup>th</sup> floors, while keeping the VE damper in 1<sup>st</sup> and 2<sup>nd</sup> floor to achieve a minimum tip deflection reduction of 25%.

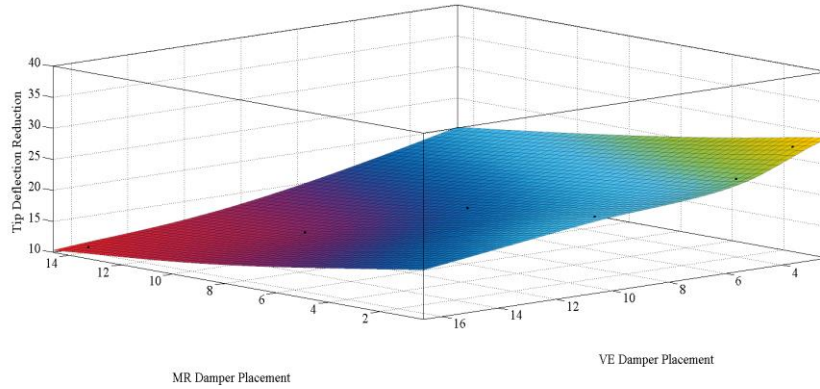


Fig. 4-6 Reduction Pattern for MR-VE combination

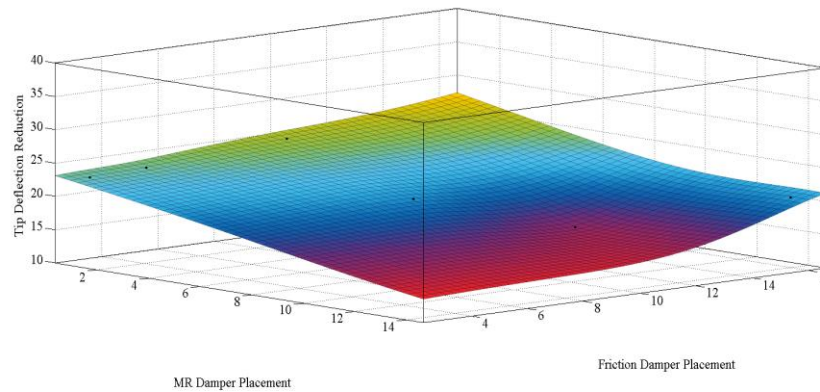


Fig. 4-7 Reduction Pattern for MR-Friction combination

**Reduction Pattern for MR-Friction combination**

General tip deflection reduction pattern is shown in Fig. 4-7 when an MR-Friction damper system is used. ‘x’ and ‘y’ axes represent the MR damper and friction damper placements respectively, while ‘z’ axis represents the tip deflection reduction percentage.

The generalized equation for the above graph can be written as

$$(x, y) = 22.89 + 6.95 \sin(1.01\pi * x * y) - 7.63e^{(-5.17y)^2} \tag{16}$$

Note: Coefficients are obtained with 95% confidence bounds

**4.1.7 Summary of findings - seismic mitigation of 18 storey structure**

Influence of the MR damper, MR and passive damper combination and their placements on seismic performance of a 18 storey steel frame under three different earthquake excitations were studied in this chapter. Reductions of seismic response parameters depend on the earthquake excitation, damper type and its placement. A comprehensive comparison has been carried out to study the effect of these parameters.

One of the main objectives of this research is to study the effect of MR damper on the seismic

mitigation of buildings. In order to compare the effectiveness of the MR damping system, results for single MR damper and two MR dampers within the building are first compared. Tip deflection reduction is first compared. Time history record of tip deflection for un-damped, single damper at 1st floor and two dampers at 1st and 3rd floor are shown in Fig. 4-8.

According to the results it can be seen an increase of tip deflection reduction with 2 MR dampers as expected. This increase has a maximum range of approximately 50%.

Tip acceleration reduction is also compared to gain a more effective comparison. Time history records of tip deflection for un-damped, single damper at 1<sup>st</sup> floor and two dampers at 1<sup>st</sup> and 3<sup>rd</sup> floors are shown in Fig. 4-9.

Average deflection reductions for the different types of damping systems and their placements under different earthquake excitations are shown in Fig. 4-10. Systems with only two dampers are used in here to achieve a more realistic comparison.

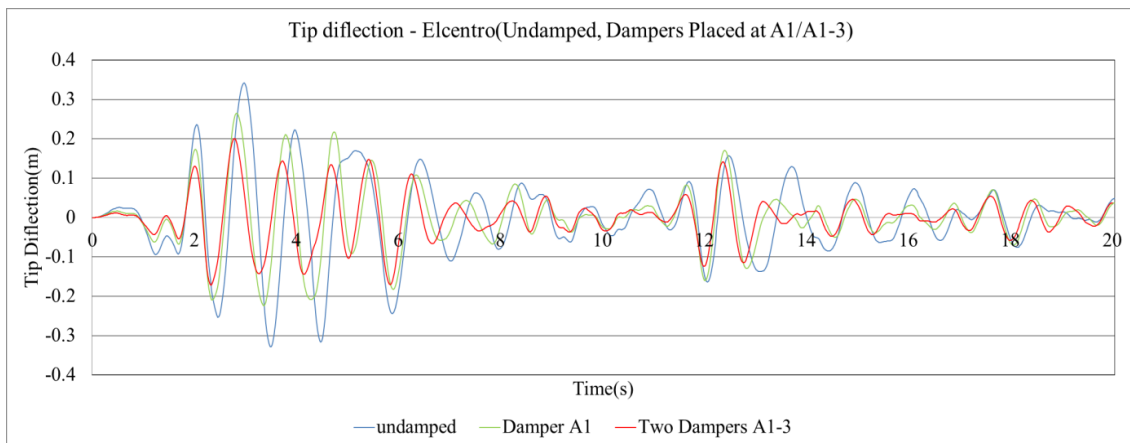


Fig. 4-8 Tip deflection comparison-single MR damper vs two MR dampers for El-Centro earthquake

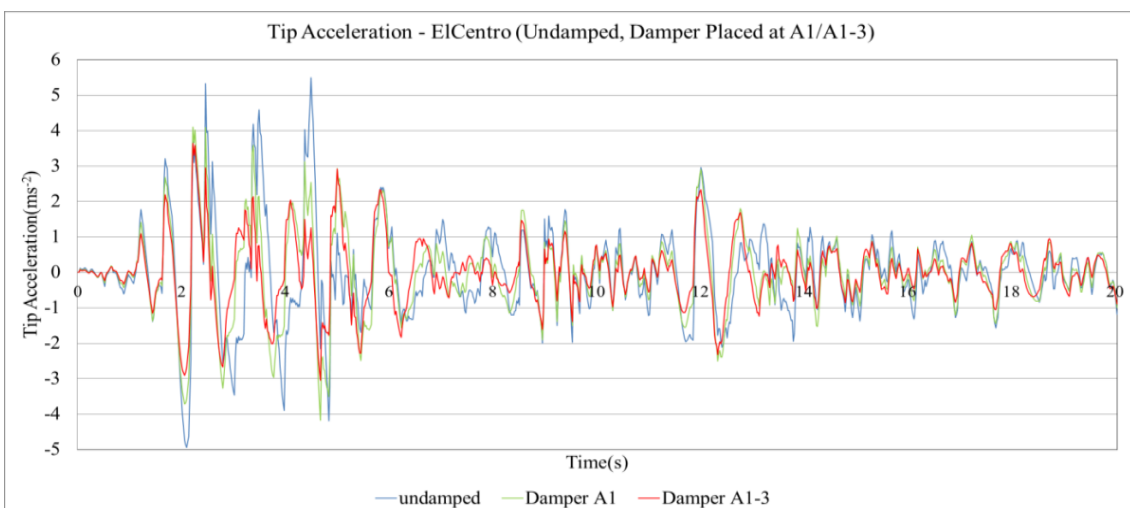


Fig. 4-9 Tip acceleration comparison-single MR damper vs two MR dampers for El-Centro earthquake

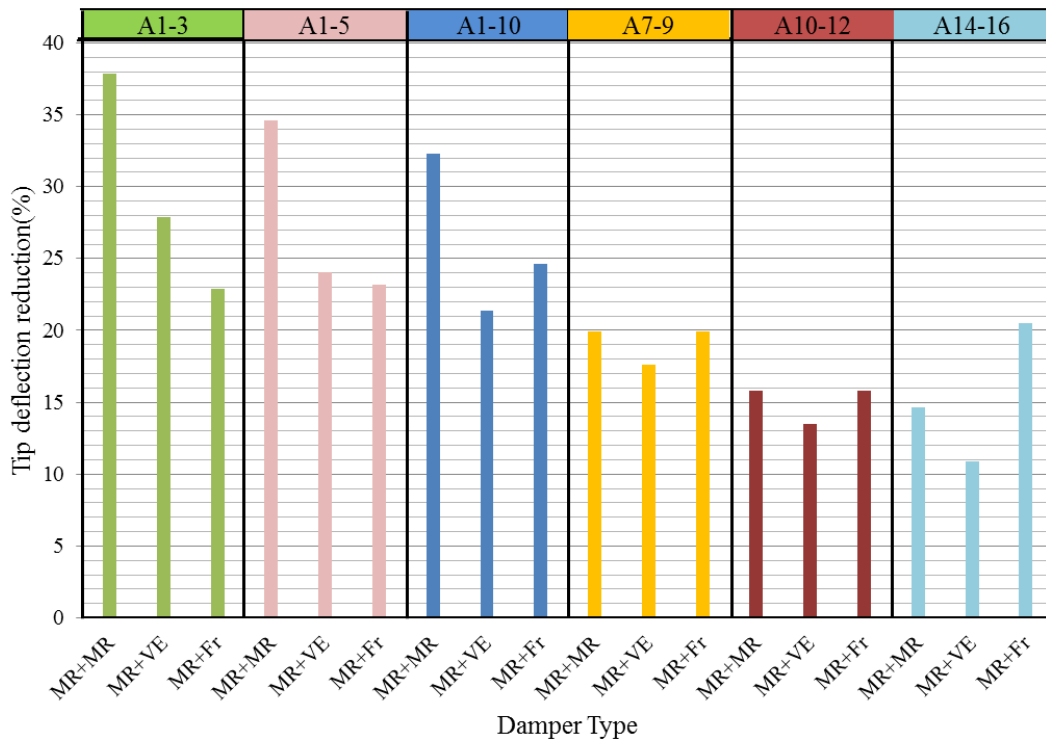


Fig. 4-10 Comparison of Tip deflection reduction for different damper types under El-Centro earthquake

Tip acceleration reduction too increased approximately by a maximum of 50% when two dampers are used. Hence, increasing of number of dampers effectively reduced the seismic response parameters, as expected. In order to study the effects of different damper systems on the seismic mitigation of the building, different damper system placed at the same locations are compared.

Overall, results show a good performance for all types of damper systems. Yet always, the highest reduction was achieved when two MR dampers were used. It has an overall reduction of 25.85%. If the average values for the second damper placement in the lower and upper floors are compared, 34.89% and 16.81% reductions in tip deflections are obtained respectively. MR-VE combination is significant when dampers are at lower floors; however performance is lower than that with 2 MR damper cases. When the VE damper is placed in the lower floors this combination has an average tip deflection reduction of 24.44% and this significantly reduces to 13.98% when the VE damper is placed in the upper floors. This again shows that VE dampers perform better when they are placed in the lower floors. MR-Friction damper combination performs better when the friction damper sits in the upper floors compared to others, and has an average tip deflection value of 18.77%. It even surpasses the performance of the 2 MR damper system. However this combination takes advantage of the single MR damper sitting on a lower floor and provides a good amount of damping. These patterns remain similar under other two earthquake records.

In addition to the previous analyses, effects of different damper locations are studied. The

average percentage tip deflection reduction for different damper locations is taken into account. Best performance is experienced in the A1-3 damper placement, with an average reduction of 29.52%. Second higher reduction occurred in A1-5. Average reduction for A1-10 damper placement is also similar to A1-5. Lowest average reduction occurs in A10-12 damper placement, 15.05%. It can be concluded that damper reduction is mainly contributed by the damper placed on the first floor.

#### 4.2 Seismic evaluation of 18 storey 3D structure

##### 4.2.1 Building structure

The building is an 18 storey structure, square on plan with 5 bays in both East-West and North-South directions. In addition to 18 storeys there are 2 basement levels below the ground for a total depth of 8 m. Bays are at 6 m centres. Each storey is 4m high, which makes the total height of the structure 72 m above the ground. Moment resisting frames provide the lateral load resistance. All column and wall base supports at the bottom of the lower basement level are idealized as pinned connections. Beams are W30×99 sections of 250 MPa steel. For columns, 0.4 m×0.4 m box columns with 5 cm thickness sections of 450 MPa steel are used.

The first three mode shapes of the building shown in Fig. 4-11 have natural frequencies of 0.56, 0.79, 0.83 Hz respectively.

##### 4.2.2 Dampers within the structure

Similar placement architecture as previously used in the analyses of the 2D models is adopted in the 3D structure. Two dampers per each frame, which makes twelve MR dampers, altogether are placed in the bottom floor. When placing dampers for MR-VE combination, six each from MR dampers and VE dampers. Damper placements are shown in Fig. 4-12. This is the plan view of the building.

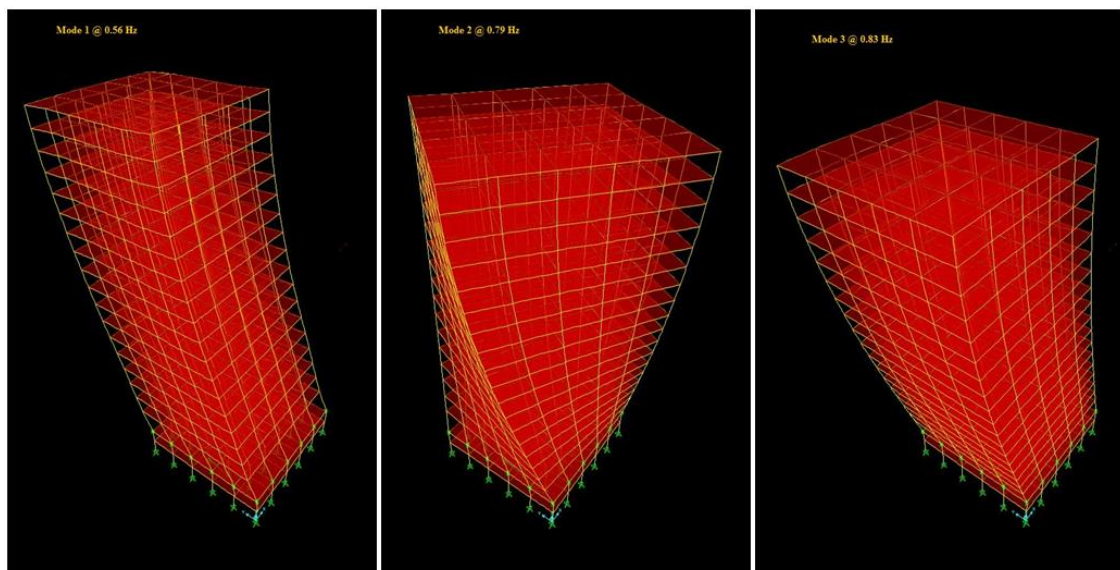


Fig. 4-11 Mode shapes of the building

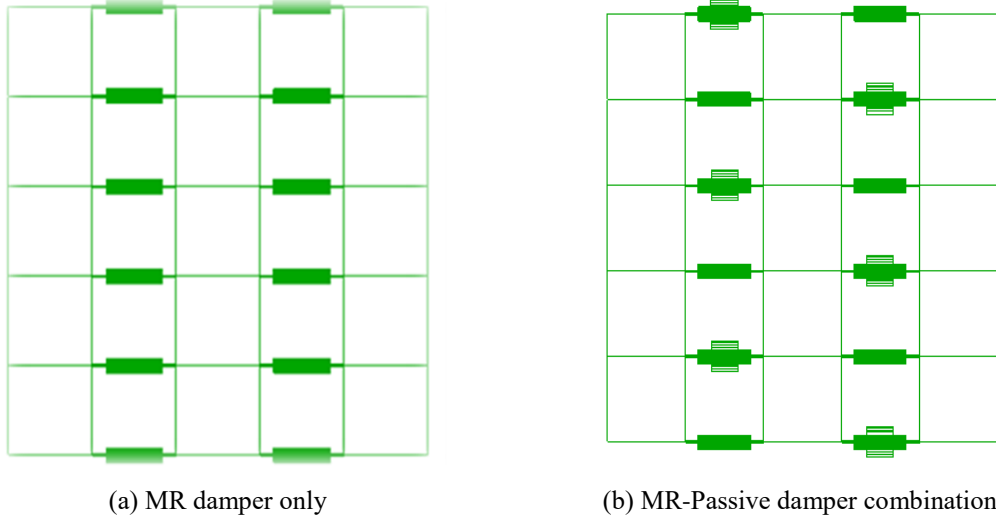


Fig. 4-12 Damper arrangement in bottom floor-Plan view

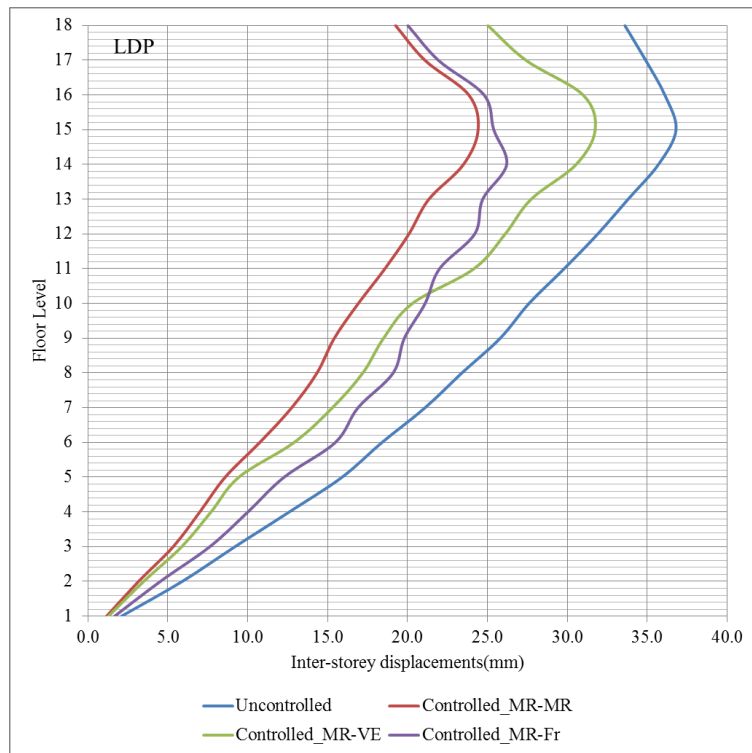


Fig. 4-13 Inter-storey drift comparison

El-Centro time history record is used as the input. Three different damper systems, MR-MR, MR-VE and MR-Friction are used in separate analyses. Inter-storey displacements (drifts) at all the floor levels are graphically presented in Fig. 4-13.

Inter-storey displacements are significantly reduced with the installation of the dampers. The MR-MR damper combination is able to achieve a noticeable reduction over other damper combinations. Average reduction with MR-MR dampers system reaches almost 40%. With MR-VE combination average reduction is 26.6% while MR-Friction damper combination maintains a 24.9% of average storey drift reduction. And it can notice MR-VE combination perform better in lower floors while MR-Friction combination works better at upper floors, as also observed in the earlier 2D analyses.

### 4.3 Seismic evaluation of 12 Storey 2D structure

MR dampers and a combination of MR and passive dampers are used for seismic mitigation of a 12 storey building structure. A 12 storey steel frame structure is considered and three main damping systems are used. The first system consists of MR dampers only. A single MR damper and two MR dampers are installed separately in the building to monitor its' seismic response. Combined MR - Viscoelastic damper system is the second system consisting of one MR damper and one VE damper. As the third one, combined MR - Friction damper system is used. Each damping system was analysed for different damper locations. Seismic analyses are performed with one damper system at one placement at a time.

#### 4.3.1 Undamped structure

The un-damped structure is also modelled and analysed. Seismic response parameters are used to compare with the damped results. Tip deflection and tip acceleration results for the un-damped structure are shown in Table 4-6.

The tip deflection and tip acceleration reductions were obtained for the structure fitted with each damper system at different locations for each of the three earthquake excitations. Then the reduction patterns were obtained according to the results, which are presented in Section 4.3.2.

#### 4.3.2 Generalized reduction patterns

Generalized seismic response reduction patterns can be modelled for this particular building and for the considered damping systems. These patterns could be used to identify the optimum damping placement and damping values for a specific damper or a damper system.

Four different reduction patterns are developed for this 12 storey structure,

1. Reduction Pattern for single MR damper
2. Reduction Pattern for two MR dampers
3. Reduction Pattern for MR-VE combination
4. Reduction Pattern for MR-Friction combination

#### Reduction Pattern for MR damper

General tip deflection reduction graph for single MR damper and two MR dampers according to its placements is shown in Fig. 4-14.

Table 4-6 Tip deflection and tip acceleration of the un-damped structure

	El Centro	Kobe	Northridge
Tip Deflection(m)	0.235	0.174	0.158
Tip Acceleration(ms <sup>-2</sup> )	5.73	6.42	5.94

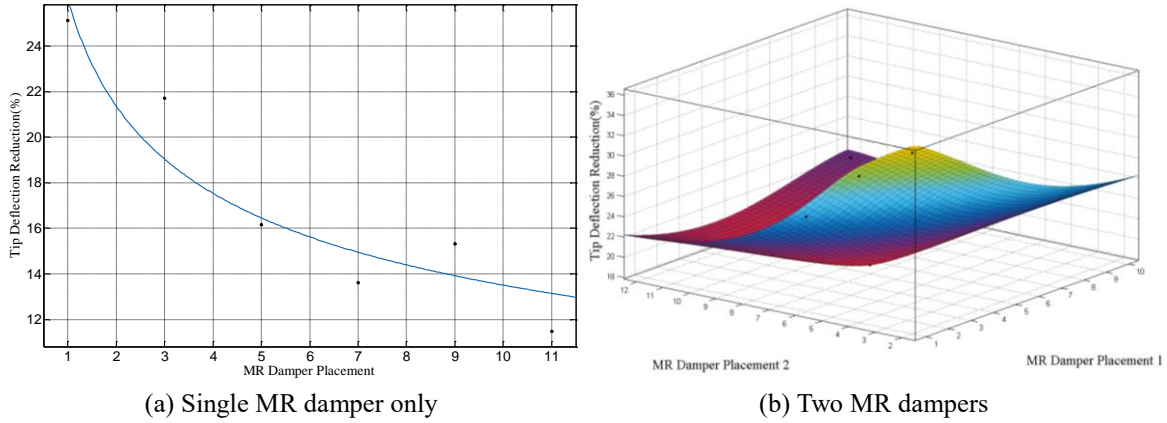


Fig. 4-14 Reduction Patterns for MR damper

Tip deflection reduction is exponentially reduced with the increase in the damper placed floor level when using a single MR damper. The generalized equation is given in Eq. (17)

$$f(x) = 16.61e^{-0.29x} \tag{17}$$

Note: Coefficients are taken with 95% confidence bounds

According to the graph, the MR damper needs to be placed in 1<sup>st</sup> of 2<sup>nd</sup> floor to achieve a 20% tip deflection reduction.

The generalized equation for the graph when two dampers are using can be given in Eq. (18)

$$f(x, y) = 0.56 + 0.7 \sin(0.18 * \pi * x * y) + 3.06e^{-(0.001y)^2} \tag{18}$$

Note: Coefficients are taken with 95% confidence bounds

According to the equation both MR dampers need to be sitting on 1<sup>st</sup> and 5<sup>th</sup> floors to achieve more than 30% tip deflection reduction.

*Reduction Pattern for damper combinations*

Generalized tip deflection reduction, with a MR damper and a passive damper is shown in Fig. 4-15.

The generalized equation for MR-VE combination according to the graph (a) is given in Eq. (19)

$$f(x, y) = 23.71 + 6.43 \sin(0.09 * \pi * x * y) - 6.16e^{-(1.59y)^2} \tag{19}$$

According to the results, MR damper can be moved between the 1<sup>st</sup> and 2<sup>nd</sup> floors, while keeping the VE damper between the 1<sup>st</sup> and 5<sup>th</sup> floor to achieve a minimum tip deflection reduction of 25%.

The generalized equation for MR-VE combination according to the graph (b) can be written as

$$f(x, y) = 23.76 - 2.67 \sin(0.77 * \pi * x * y) - 16.75e^{-(4.09y)^2} \tag{20}$$

Note: Coefficients are taken with 95% confidence bounds

To gain a minimum tip deflection reduction of 25%, MR damper needs to be installed between the first six floors while the friction damper installed between 1<sup>st</sup> and 5<sup>th</sup> floors or 10<sup>th</sup> and 12<sup>th</sup>

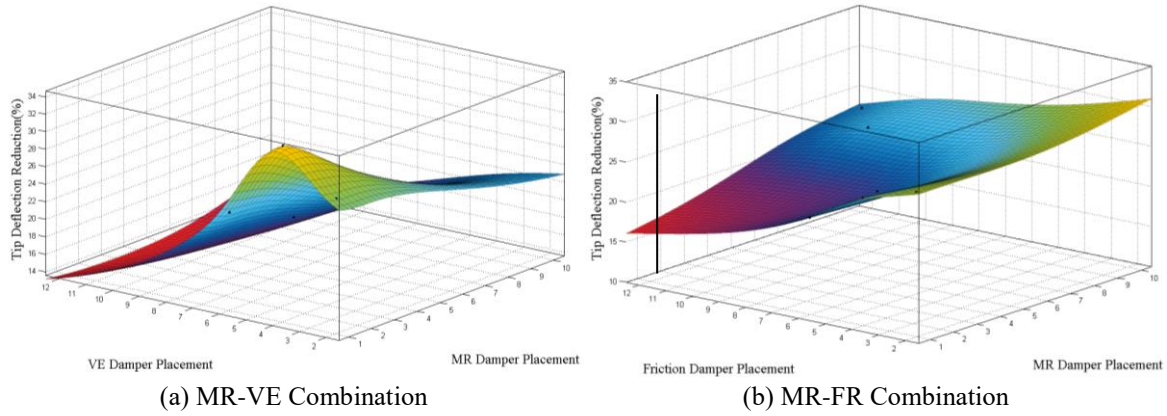


Fig. 4-15 Reduction Pattern for MR-VE combination

floors. At the lower floors a great deal of damping occurs due to the MR damper. The damper combination acts to reduce the tip deflection, only when placed in the upper floors.

**4.3.3 Summary of findings - 12 Storey structure**

Influence of the MR damper, MR and passive damper combinations and their placements on seismic performance of a 12 storey steel frame under three different earthquake excitations were studied in this chapter. Reductions of seismic response parameters greatly depend on the

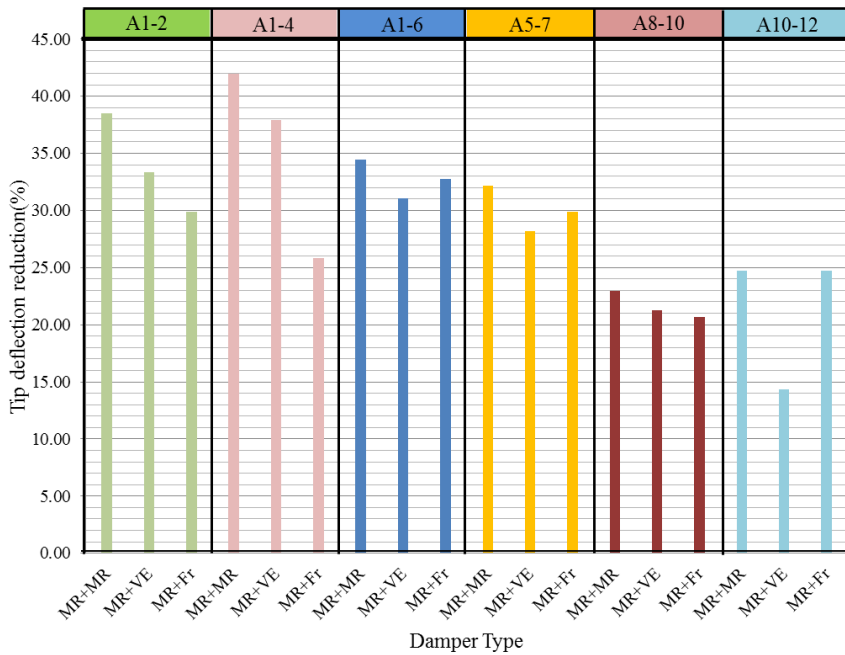


Fig. 4-16 Comparison of Tip deflection reduction for different damper types under Kobe earthquake

earthquake excitation, damper type and its placement. A comprehensive evaluation has been carried out to compare the performances and to study the effect on the seismic mitigation parameters.

In order to study the effect of the different damper systems, seismic responses of the structure with the different damper systems for the same placement are compared. Average tip deflection reductions for the different types of damping systems and their placements under Kobe earthquake excitations are shown in Fig. 4-16. Only systems with two dampers are used in here to achieve a more realistic comparison.

In the first three cases where one of the MR dampers sits on the first floor, seismic mitigation of the tip deflection reduction of more than 30% is obtained. When both dampers move to the upper floors this value has reduced to an average of 20%. These results confirm that MR dampers perform better in the lower floors of the building.

Similar to the MR-MR system, MR-VE system too shows a better mitigation when both dampers are placed in the lower floors. But, the MR-MR system shows higher mitigation compared to the MR-VE system. When both dampers move to the upper floors the average mitigation has reduced to 20-25%. MR-Fr combination shows a relative steady pattern; though MR damper performance is reduced at upper floors, the friction damper balances that by increased performance in the upper floors.

Overall results show that good seismic mitigation can be obtained with all the damper systems considered in this study. Depending on the amount of mitigation requires, the appropriate damper system can be selected and placed at the particular locations. In all cases, the highest mitigation was achieved when two MR dampers were used. It has an overall reduction of more than 35% when both dampers are placed in the lower floors. MR-VE combination is significant when dampers are at lower floors, however the mitigation provided is lower than that with 2 MR dampers. In the lower floors it has an average of approximately 30%. It significantly reduces to around 15% when placed in the upper floors. This confirms that VE dampers perform better when they are placed in the lower floors. MR-Friction damper combination performs better when the friction damper sits in the upper floors, and has an approximate mitigation value (with respect to tip deflection reduction) of 25%. It even surpasses the 2 MR dampers system. However this combination does takes the advantage of the MR damper placed in the lower floor. This pattern remains the same for all three earthquakes considered.

## **5. Conclusions**

This research developed and applied a procedure for using MR damper systems, combined MR-VE damper systems and MR-friction damper systems to mitigate the seismic effects of building structures. These damper systems are placed at different floor levels. Three earthquake excitations namely, El-Centro, Kobe and Northridge are selected as inputs. Results for tip deflection, tip acceleration and inter-storey drift are compared.

According to the analysis results it can be concluded that the MR damper performs well in seismic mitigation of the 18 storey 2D and 3D structure. When two MR dampers are used, both tip deflection and tip accelerations had higher reductions compared those obtained with MR-Passive damper combinations. Tip deflection reduction achieved an average value of 35% when two MR dampers were placed in the lower floors. MR-VE combination provided the best results when both dampers are attached to the lower floors, providing a tip deflection reduction of approximately

25%. For MR-Friction combination, friction damper needed to be fixed in the upper floors in order to provide an effective reduction. However, the MR damper dominates the reduction in tip deflection. This research generated a vast amount of information which was used to develop general reduction patterns for different damper combinations. These patterns could be used to find the optimum damping combination according to the expected damping reduction requirement.

Overall results of 12 story structure also showed that good seismic mitigation can be obtained with all the damper systems considered in the study. Depending on the amount of mitigation required, the appropriate damper system can be selected and placed at the particular locations. It can be observed that both tip deflection and tip acceleration reduced by a greater margin when MR-MR combination was used specially in lower floors. MR-VE combination was significant when dampers are at the lower floors; however the mitigation provided was lower than that with 2 MR dampers. In the lower floors it has an average of approximately 30%. It significantly reduces to around 15% when placed in the upper floors. This confirms that VE dampers perform better when they are placed in the lower floors. MR-Friction damper combination performs better when the friction damper sits in the upper floors, and has an approximate mitigation value (with respect to tip deflection reduction) of 25%. It even surpasses the 2 MR dampers system. However, this combination takes the advantage of the MR damper placed in the lower floor. This pattern remains the same for all three earthquakes considered. Finally, general reduction patterns have been developed which could be used to find the optimum damping combination according to the expected damping reduction requirement for this type of a building.

It can be concluded that magneto-rheological (MR) damper has a better ability, than the passive dampers, to control the dynamic response of building structures during earthquakes. Further, MR damper increases the damping property of a structure adaptively without changing the natural frequencies of the structure. It is found that the performance of the damper is sensitive to the location of the damper placement and optimum location is at the ground floor in all cases.

Generally, determining the type of damping devices and their optimal placement remains a highly iterative trial and error process. This research suggests the development of "Generalized Reduction Patterns" for different damper types and their locations. The mitigation under two types of dampers can be plotted against the height of the building, as illustrated in this research. Optimal damper placement and type can be found accordingly. These reduction patterns for distinct buildings will help to find optimum placements of dampers and their combinations.

## References

- Abbas, H. and Kelly, J.M. (1994), "A methodology for design of viscoelastic dampers in earthquake-resistant structures", Earthquake Engineering Research Center, University of California.
- Amini, F. and Javanbakht, M. (2014), "Simple adaptive control of seismically excited structures with MR dampers", *Struct. Eng. Mech.*, **52**(2), 275-290.
- Craig, R.R. and Yung-Tsen, Y.-T. (1982), "Generalized substructure coupling procedure for damped systems", *AIAA J.*, **20**(3), 442-444.
- CSI. (2013), *Computers and Structures Inc.*, Berkeley, CA, USA.
- Das, D., Datta, T. and Madan, A. (2012), "Semiactive fuzzy control of the seismic response of building frames with MR dampers", *Earthq. Eng. Struct. Dyn.*, **41**(1), 99-118.
- Dyke, S.J., Jr, B.F.S., Carlson, M.K.S. and Carlson, J.D. (1996), "Modeling and control of magnetorheological dampers for seismic response reduction", *Smart Mater. Struct.*, **5**(5), 565-575.
- Hao, L. and Zhang, R. (2016), "Structural safety redundancy-based design method for structure with viscous

- dampers”, *Struct. Eng. Mech.*, **56**(4), 821-840.
- Lee, J. and Kim, J. (2015), “Seismic performance evaluation of moment frames with slit-friction hybrid dampers”, *Earthq. Struct.*, **9**(6), 1291-1311.
- Marko, J., Thambiratnam, D. and Perera, N. (2004), “Influence of damping systems on building structures subject to seismic effects”, *Eng. Struct.*, **26**(13), 1939-1956.
- Metwally, H., El-Souhily, B. and Aly, A. (2006), “Reducing vibration effects on buildings due to earthquake using magneto-rheological dampers”, *Alexandria Eng. J.*, **45**(2), 131-140.
- Ogata, Y. (2010), “Space-time heterogeneity in aftershock activity”, *Geophys. J. Int.*, **181**(3), 1575-1592.
- Spencer Jr, B. and Nagarajaiah, S. (2003), “State of the art of structural control”, *J. Struct. Eng.*, **129**(7), 845-856.
- TheMathWorksInc. (2014), MATLAB.
- Tseng, H. and Hedrick, J. (1994), “Semi-active control laws-optimal and sub-optimal”, *Vehicle Syst. Dyn.*, **23**(1), 545-569.
- Wilson, E.L. (1997), “SAP2000: integrated finite element analysis and desing of structures”, *Analysis reference: Computers and Structures*.